Reaction Chemistry & Engineering

ROYAL SOCIETY OF CHEMISTRY

PAPER

View Article Online
View Journal | View Issue

Cite this: *React. Chem. Eng.*, 2021, **6**, 1878

Surface engineering of a Cu-based heterogeneous catalyst for efficient azide–alkyne click cycloaddition

Gianvito Vilé, *[a] Jiaxu Liu [b] and Zhenmei Zhang[b]

Received 19th May 2021,
Accepted 6th July 2021

DOI: 10.1039/d1re00199j

rsc.li/reaction-engineering

In this work, we disclose that atomic-scale engineering of the active sites in copper-based catalysts can effectively tune the material performance for regioselective synthesis of triazoles, important building blocks for fine chemicals and pharmaceuticals. The copper catalysts have been prepared *via* impregnation of β zeolites with a Cu precursor, followed by post-synthetic modification with an organic ligand. The ligand is expected to partially cover the active sites, reducing the ensemble where the reaction takes place. The materials have been characterized by nitrogen adsorption, TEM, XRD, SEM-EDX, and FTIR spectroscopy to determine the structural, compositional, and textural properties of the samples. Catalyst testing in a one-pot three-component reaction of organic halides, terminal alkynes, and sodium azides in water shows that the presence of an organic layer on the catalyst surface favours the reaction. Leaching experiments in eight successive cycles have been conducted to prove the stability of the materials.

Introduction

The design at the atomic scale of innovative catalytic materials is an increasingly important direction for sustainable chemical synthesis.[1] Catalytic materials are used in more than 80% of all chemical processes.[2] In particular, within the pharmaceutical sectors, homogeneous catalysts in the form of organometallic complexes, inorganic acids, and soluble salts are often employed. The underlying question when evaluating process improvement strategies is whether it is meaningful to heterogenize a catalyst that is active and selective under homogeneous conditions. Despite skepticism from the community, numerous examples of heterogeneous catalysts for reactions traditionally conducted over homogeneous systems have been reported to date.[3]

The Cu-catalyzed triazole synthesis is among those reactions that can benefit for an improved understanding of the catalyst structure. Developed by Huisgen and Sharpless,[4] this method is importantly applied in the regioselective synthesis of substituted triazoles, building blocks to make drugs, perfumes, and vegetable essences, as well as versatile intermediates for modern life science technologies.[5] Enormous efforts have been devoted to maximizing the general efficiency of this reaction, which is homogeneously catalyzed using copper(I) complexes.[6] In fact, the presence of a significant amount of copper species in the final product (requiring costly methods for metal recovery and product purification) remains a challenge hampering the large-scale utilization of the technology.[7] In this context, some authors have reported stable poly(*N*-vinyl-2-pyrrolidone) (PVP)-protected copper nanoparticles as effective homogeneous catalysts for 1,3-dipolar cycloaddition of alkynes and azides to obtain 1,2,3-triazoles, with excellent yields under mild reaction conditions. These nanocatalysts could be recycled and reused several times without significant loss of metal.[8] However, the need for expensive organic precursors and reducing agents makes this approach less industrially attractive.

To overcome these limitations, heterogeneous catalysts based on the exploitation of copper oxide nanoparticles have been recently developed.[9] In particular, it has been shown that Cu_2O nanoparticles are more efficient for synthesizing both aliphatic and aromatic azides and are less toxic than the commonly-used homogeneous $CuSO_4$/reductant systems.[10] Besides, the possibility to immobilize these nanoparticles on heterogeneous carriers enables the reutilization of the same material for consecutive reactions, an aspect which meets the requirement for circular economy.

Despite the attractivity of such approaches, the relationship between the ensemble of the active site in immobilized copper oxide nanoparticles and the catalytic performance has not been elaborated. Building on these contributions, this work studies how the control of the active

[a] *Department of Chemistry, Materials and Chemical Engineering "Giulio Natta", Politecnico di Milano, Piazza Leonardo da Vinci 32, 20133 Milano, Italy. E-mail: gianvito.vile@polimi.it*
[b] *State Key Laboratory of Fine Chemicals, Department of Catalytic Chemistry and Engineering, Dalian University of Technology, Ganjingzi District, Linggong Road, 2116024 Dalian, China*

site *via* post-synthetic modification of copper nanoparticles can enhance the catalyst reactivity and selectivity. This offers an improved understanding of the optimal catalysts based on the exploitation of Cu_2O nanoparticles, and can further drive the design of catalytic materials for triazole synthesis.

Materials and methods

Catalyst preparation

NH_4-β zeolites (with a total Si/Al ratio of 120) were supplied by the Dalian Ligong Qiwangda Chemical Technology Company. Hβ zeolite (herein, indicated as β) was obtained from the calcination of NH_4-β zeolites under dry air at 540 °C for 6 h. The incorporation of Cu was performed by incipient wetness impregnation. In particular, 1.0 g of this material was added to 0.47 mL of a 0.5 mol L^{-1} aqueous solution of $Cu(NO_3)_2{\cdot}3H_2O$ (Sigma-Aldrich) and stirred at 60 °C for 3 h. Afterwards, the solid was dried at 60 °C for 6 h, and calcined at 550 °C for 3 h to obtain nano-Cu/β.

The post-synthetic modification of nano-Cu/β to obtain a hybrid Cu-based catalyst (hybrid-Cu/β) was performed by following an established method for the surface modification of copper oxide and using a commercial and cheap surfactant.[11] In particular, 1 g of nano-Cu/β was immersed in 50 mL of 10^{-3} mol L^{-1} *n*-dodecylphosphonic acid (Alfa Aesar) in ethanol, and the suspension was kept in a closed vial, at room temperature and under stirring for 24 h. Then, the modified copper sample was filtered, subjected to 10 min sonication in ethanol, and finally dried at 60 °C for 6 h.

Catalyst characterization

To determine the bulk Si/Al ratio and the elemental Cu content, the materials were analyzed by X-ray fluorescence (XRF) on a Bruker SRS3400 spectrometer (Bruker, Madison, USA). The X-ray diffraction (XRD) patterns of the powders were recorded using a Rigaku D/max – 2004 diffractometer (Rigaku, Kyoto, Japan) with Cu Kα radiation (40 kV, 100 mA) and a 0.01° min^{-1} (2θ) scanning speed. Transmission electron microscopy (TEM) was done on an FEI (Tecnai F30 G2, The Netherlands) microscope. Nitrogen physisorption was conducted on a Micromeritics ASAP 3020 instrument (Micromeritics, Atlanta, USA) at −196 °C. Before data collection, the samples (*ca.* 20–40 mesh) were degassed at 120 °C for 6 h. The surface area was determined by the Brunauer–Emmett–Teller (BET) method using the adsorption branch in the p/p_0 range from 0.05 to 0.35. The micropore and mesopore volumes were calculated using the *t*-plot method at p/p_0 of 0.99. Fourier transform infrared spectroscopy (FTIR) was used to investigate the acid sites of the zeolite catalysts. The spectra for surface hydroxyl (OH) vibrations and pyridine adsorption were recorded with a Nicolet 10 FT-IR spectrometer in the range from 4000 to 400 cm^{-1} with an optical resolution of 4 cm^{-1}. The zeolite sample (16 mg) was pressed into a self-supporting thin wafer and decontaminated at 120 °C under vacuum (10^{-3} Pa) for 6 h in a quartz IR cell equipped with CaF_2 windows. Afterwards, the cell was cooled down to room temperature for sample measurement. The hydroxyl vibration spectra were measured by subtracting the background spectrum (recorded with an empty IR cell in the absence of the sample) from the measured sample spectra.

Catalyst performance

In a pressure-resistant tube, alkyl halide (0.5 mmol), sodium azide (0.5 mmol), and alkyne (0.5 mmol) were dissolved in 3.0 mL of water, and the catalyst (30 mg) was added. The reaction tube was sealed and heated in an oil bath at 70–110 °C for 0–10 h. After the completion of the reaction, the crude product was extracted from the catalyst by washing with ethyl acetate. For the stability test, the catalyst was washed with ethyl acetate, water, and ethanol, dried at 60 °C for 6 h, and reused in a subsequent reaction run.

Results and discussion

Catalyst characterization

The parent β has a BET surface area of 678 m^2 g^{-1} and a pore volume of 0.28 m^2 g^{-1}. The BET surface area and the pore volume slightly decrease after Cu incorporation, becoming 653 m^2 g^{-1} and 0.23 m^2 g^{-1}, respectively (Table 1 and Fig. 1a). After grafting, the hybrid sample has a BET area of 564 m^2 g^{-1} and a pore volume of 0.20 m^2 g^{-1} (Fig. 1a). From these data, we can conclude that both nano-Cu/β and hybrid-Cu/β have comparable textural properties. The X-ray diffraction (XRD) patterns of the different samples in the 5–40 2θ region is shown in Fig. 1b. These patterns exhibit prominent diffraction peaks at 7.8°, 21.6°, 22.6°, 25.3°, 27.0°, and 29.6°, which are characteristic for β-type zeolite.[12] As expected, the samples are thus highly crystalline. A peak at 43° is present, which can be indexed with the (200) lattice fringe of Cu_2O.[13] The small intensity of this peak is due to the high dispersion of the copper phase. This is verified by microscopy analysis. Fig. 2 shows the transmission electron micrographs of nano-Cu/β. The parent zeolite particles have well-defined cubic shapes. On top, small (5–10 nm) copper oxide species are well dispersed.

Fourier-transform infrared (FTIR) spectroscopy (Fig. 1c) was performed to study the hydroxyls (–OH) related to Brønsted acidity and those representatives of isolated silanols on the external surface in the materials.[14] Both Cu-based catalysts display a small band at 3610 cm^{-1} related to the Brønsted acidity[15] and a prominent band at 3741 cm^{-1}, characteristic of isolated SiOH.[16] However, the intensity of these bands is similar for both samples, which indicate that the resultant catalytic differences cannot be attributed to variation in the acid character of the carrier. Finally, XRF analysis of nano-Cu/β and hybrid-Cu/β confirms that both catalysts have a Cu loading of 1.5 wt% (Table 1).

Table 1 reports the P/Cu ratio over the samples. On the nano-Cu/β, no phosphorus is detected. On the other hand,

Table 1 Textural and surface properties of the samples

Catalyst	S_{BET}[a]/m^2 g^{-1}	V_{pore}[b]/cm^3 g^{-1}	Cu[c]/wt%	P/Cu$_{obs}$[d]/—
Nano-Cu/β	653	0.23	1.5	0
Hybrid-Cu/β	564	0.20	1.5	0.082

[a] From BET method. [b] From the *t*-plot method. [c] From X-ray fluorescence spectroscopy. [d] Relative atomic concentration of P/Cu, proving the presence of ligand on the surface of the copper oxide nanoparticles in hybrid-Cu/β.

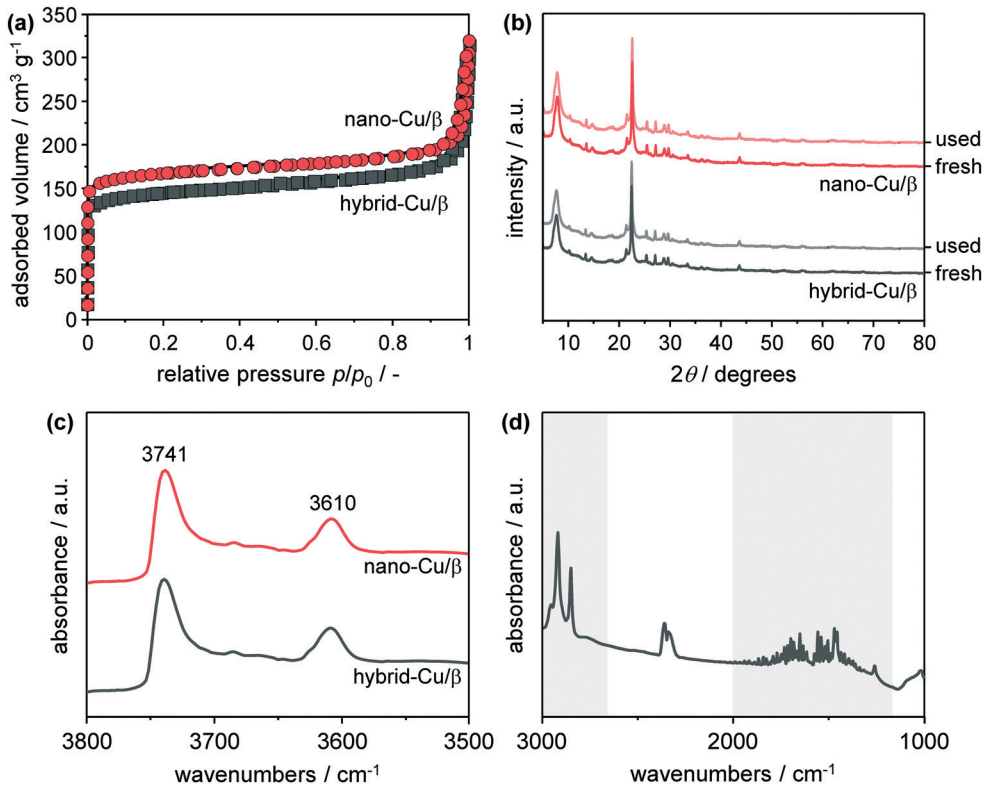

Fig. 1 N_2 adsorption–desorption isotherms (a), X-ray diffraction patterns (b), and FTIR spectra (c and d) of the samples.

the corresponding values over hybrid-Cu/β is 0.082.[14] This parameter confirms the presence of the ligand on the hybrid-Cu/β, and can be used to evaluate the grafting efficiency of our route. In fact, based on the recipe reported in the Materials and methods, 0.237 mmol Cu is present on the catalyst after incipient wetness impregnation, assuming full impregnation of the 0.47 mL aqueous solution of $Cu(NO_3)_2{\cdot}3H_2O$ at 0.5 mol L^{-1} concentration. On the other hand, the *n*-dodecylphosphonic acid solution used for ligand grafting contains 0.048 mmol of ligand, given the 1 : 1 stoichiometry between P and *n*-dodecylphosphonic acid ($C_{12}H_{27}O_3P$). Based on the theoretical P/Cu ratio determined here (P/Cu$_{theor}$ = 0.201) and on the experimentally obtained result (P/Cu$_{obs}$ = 0.082), we can estimate a grafting efficiency of 41%, which is in line with literature precedents.[11] Fig. 1d shows the infrared spectra of the hybrid catalyst in the 3000–1000 cm^{-1} region, confirming the presence of the ligand over hybrid-Cu/β. Several IR reflections in the 1000–2000 cm^{-1} are indexed to P–O and P═O vibrations. Meanwhile, the peaks at *ca.* 2850 and 2919 cm^{-1} correspond to highly-ordered and self-organized alkane chains entrapped on the catalyst surface, as shown elsewhere.[14] From these data, it is difficult to determine the preferential grafting mode (mono, bi, or tridentate) of *n*-dodecylphosphonic acid on the surface of Cu_2O, although earlier results have demonstrated that bidentate grafting seems comparable for copper oxide catalytic surfaces.[11,17]

Catalyst performance

With the full set of characterization techniques in hands, we have initiated the catalytic evaluation of the samples, using first the synthesis of 1,4-disubstituted-1,2,3-triazole *via* the 1,3-dipolar cycloaddition between phenylacetylene and the organic azide formed *in situ* from the corresponding benzyl bromide and sodium azide. The reaction was first conducted at 110 °C. Increasing the reaction time (Fig. 3a), the yield of 1,4-disubstituted-1,2,3-triazole increases with both catalysts.

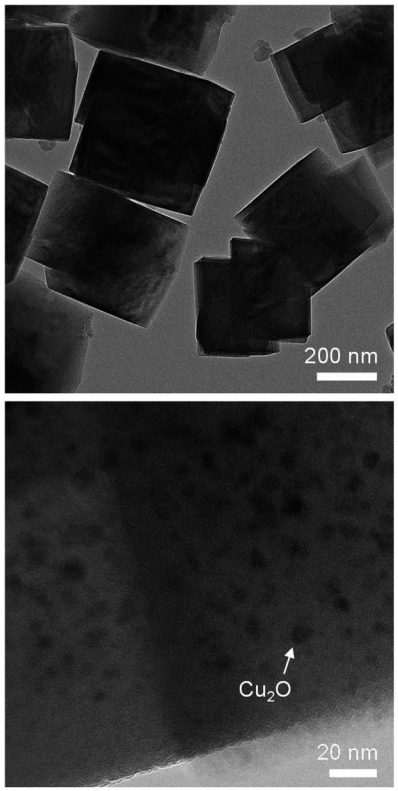

Fig. 2 Transmission electron micrographs of nano-Cu/β.

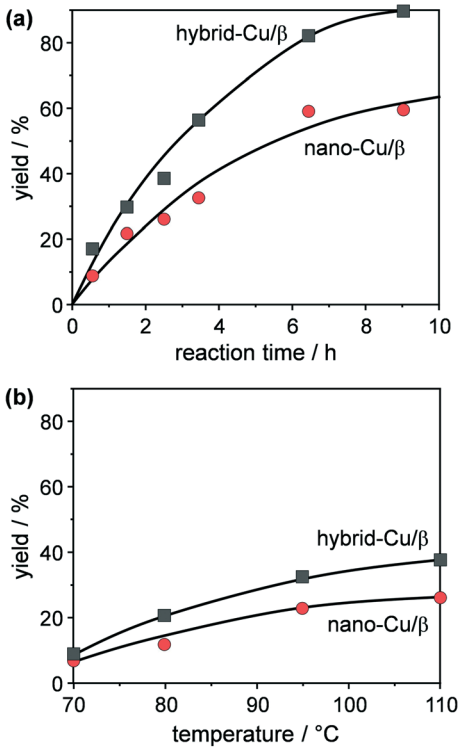

Fig. 3 Effect of reaction time (a, at a fixed temperature of 110 °C) and temperature (b, at a fixed reaction time of 2.5 h) on the conversion of 1,4-disubstituted-1,2,3-triazole *via* 1,3-dipolar cycloaddition between phenylacetylene, benzyl bromide, and sodium azide. Each experimental data was collected using 0.5 mmol benzyl bromide, 0.5 mmol sodium azide, 0.5 mmol phenylacetylene, 3.0 mL water, and 30 mg catalyst.

However, hybrid-Cu/β appears to be more reactive than nano-Cu/β. In fact, after a 2.5 h reaction time, the yield of 1,4-disubstituted-1,2,3-triazole is 25% over nano-Cu/β and *ca.* 40% over hybrid-Cu/β. With a longer reaction time (>7 h), the formation of 1,4-disubstituted-1,2,3-triazole using the nano-Cu/β catalyst reaches a plateau at *ca.* 60%, while the use of hybrid-Cu/β results in 90% isolated yield. This result is confirmed keeping the reaction time constant at 2.5 h, and varying the temperature from 70 °C to 110 °C (Fig. 3b). Also in this case, the hybrid-Cu/β catalyst leads to a higher fraction of the formed product compared to the nano-Cu/β catalyst under all conditions.

It must be noted that both catalysts have similar textural and surface properties. Thus, all differences must be linked to the surface modification on the copper oxide nanoparticle induced by the presence of *n*-dodecylphosphonic acid. Modification of the copper surface by incorporation of a phosphonate-terminated film reduce the active sites formed by the copper ensemble, since the monolayer film induce separation of the copper surface metal center.[18] Based on the catalysis data, this appears to be desirable to better control the active site and enhance the reactivity.

The durability of the hybrid-Cu/β was investigated by employing it in several successive reactions (Fig. 4). After the first cycle, the material was recovered and reused in a subsequent reaction. It is noteworthy to mention that no distinct difference in the yield of the product was observed and the catalytic system worked extremely well even up to eight subsequent runs. ICP-MS analysis of the product solution after the runs confirmed the absence of any leached Cu species in the sample.

To finally expand the applicability of this procedure, several alkynes and azides with different functionalities were examined (Table 2). The reaction works well with a variety of

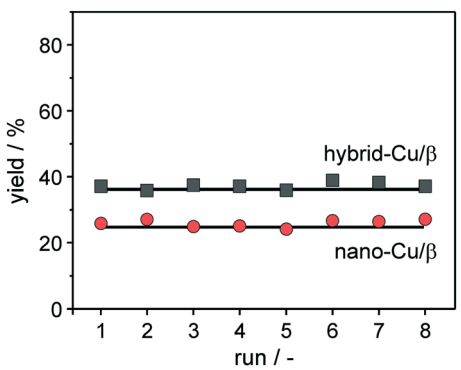

Fig. 4 Evaluation of the recyclability of the nano-Cu/β and hybrid-Cu/β. Each experimental data was collected using 0.5 mmol benzyl bromide, 0.5 mmol sodium azide, 0.5 mmol phenylacetylene, 3.0 mL water, and 30 mg catalyst, using a temperature of 110 °C and a reaction time of 2.5 h.

Table 2 Substrate scope for the synthesis of 1,4-disubstituted-1,2,3-triazoles over nano-Cu/β and hybrid-Cu/β. Each experimental data was collected using 0.5 mmol alkyl halide, 0.5 mmol sodium azide, 0.5 mmol alkyne, 3.0 mL water, and 30 mg catalyst, using a temperature of 110 °C and a reaction time of 9 h

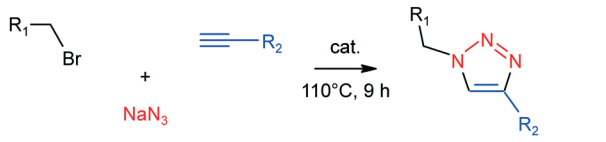

			Yield (%)	
Entry	R_1	R_2	Nano-Cu/β	Hybrid-Cu/β
1	Ph	Ph	58	90
2	4-Br-Ph	Ph	51	87
3	2-Br-Ph	Ph	48	93
4	4-NO_2-Ph	Ph	43	81
5	2,2-Cl-Ph	Ph	48	78
6	2,4-Cl-Ph	Ph	44	79
7	Ph	2-Me-Ph	46	92
8	Ph	4-Br-Ph	38	91
9	Ph	*n*-C_4H_9	41	69
10	Ph	4-NO_2-Ph	46	87

aryl halides (entries 1–6) and alkynes (entry 7–10), tolerating a wide spectrum of electron donating and withdrawing functional groups in the starting material.

Conclusions

A novel catalyst based on a surface-modified Cu-based β-zeolite has been reported. The catalyst has proven to be highly active for the one-pot copper-catalyzed alkyne–azide cycloaddition, providing the expected triazoles in better yields compared to the bare Cu_2O-based catalyst. Moreover, the reactions could be performed using water as solvent, which is advantageous in terms of process sustainability. The catalyst could be efficiently recycled and reused at least 8 times without marked loss in its activity and with neglectable metal leaching in the liquid phase.

Conflicts of interest

There are no conflicts to declare.

Acknowledgements

GV thanks Carola Romani for support during material characterization and for performing catalytic experiments. Fondazione Bracco, Bracco Imaging, and Politecnico di Milano are acknowledged for funding.

Notes and references

1 (*a*) B. Van Vaerenbergh, J. Lauwaert, P. Vermeir, J. W. Thybaut and J. De Clercq, *React. Chem. Eng.*, 2020, **5**, 1556–1618; (*b*) S. Siahrostami, S. Jimenez Villegas, A. Hassan Bagherzadeh Mostaghimi, S. Back, A. Barati Farimani, H. Wang, K. Aslaug Persson and J. Montoya, *ACS Catal.*, 2020, **10**, 7495–7511; (*c*) P. Han, S. Axnanda, I. Lyubinetsky and D. W. Goodman, *J. Am. Chem. Soc.*, 2007, **129**, 14355–14361; (*d*) P. Sharma, S. Kumar, O. Tomanec, M. Petr, J. Z. Chen, J. T. Miller, R. S. Varma, M. B. Gawande and R. Zbořil, *Small*, 2021, **17**, 2006478.

2 Y. Xia, C. T. Campbell, B. R. Cuenya and M. Mavrikakis, *Chem. Rev.*, 2021, **121**, 563–566.

3 (*a*) M. Di Serio, M. Cozzolino, M. Giordano, R. Tesser, P. Patrono and E. Santacesaria, *Ind. Eng. Chem. Res.*, 2007, **46**, 6379–6384; (*b*) Q. Sun, Z. Dai, X. Meng, L. Wang and F.-S. Xiao, *ACS Catal.*, 2015, **5**, 4556–4567; (*c*) X. Cui, W. Li, P. Ryabchuk, K. Junge and M. Beller, *Nat. Catal.*, 2018, **1**, 385–397; (*d*) S. Neumann, M. Biewend, S. Rana and W. H. Binder, *Macromol. Rapid Commun.*, 2020, **41**, 1900359.

4 (*a*) R. Huisgen, *Pure Appl. Chem.*, 1989, **61**, 613; (*b*) H. C. Kolb, M. G. Finn and K. B. Sharpless, *Angew. Chem., Int. Ed.*, 2001, **40**, 2004.

5 (*a*) F. Gao, A. Hunter, S. Qu, J. R. Hoffman, P. Gao and W. A. Phillip, *ACS Nano*, 2019, **13**, 7655; (*b*) P. Zhang, T. Yamamoto and M. Suginome, *ChemCatChem*, 2019, **11**, 424; (*c*) J. Wen, K. Wu, D. Yang, J. Tian, Z. Huang, A. S. Filatov, A. Lei and X.-M. Lin, *ACS Appl. Mater. Interfaces*, 2018, **10**, 25930.

6 (*a*) C. Yang, J. P. Flynn and J. Niu, *Angew. Chem., Int. Ed.*, 2018, **57**, 16194; (*b*) C. Barner-Kowollik, F. E. Du Prez, P. Espeel, C. J. Hawker, T. Junkers, H. Schlaad and W. Van Camp, *Angew. Chem., Int. Ed.*, 2011, **50**, 60; (*c*) F. Liu, H. Wang, S. Li, G. A. L. Bare, X. Chen, C. Wang, J. E. Moses, P. Wu and K. B. Sharpless, *Angew. Chem.*, 2019, **131**, 8328; (*d*) B. Zhao, Z. Gao, Y. Zheng and C. Gao, *J. Am. Chem. Soc.*, 2019, **141**, 4541; (*e*) S. Roy, T. Chatterjee, M. Pramanik, A. Singha Roy, A. Bhaumik and S. M. Islam, *J. Mol. Catal. A: Chem.*, 2014, **386**, 78; (*f*) S. Elavarasan, A. Bhaumik and M. Sasidharan, *ChemCatChem*, 2019, **11**, 4340.

7 (*a*) A. Cano-Odena, P. Vandezande, D. Fournier, W. Van Camp, F. E. Du Prez and I. F. J. Vankelecom, *Chem. – Eur. J.*, 2010, **16**, 1061–1067; (*b*) C. J. Pickens, S. N. Johnson, M. M. Pressnall, M. A. Leon and C. J. Berkland, *Bioconjugate Chem.*, 2018, **29**, 686–701.

8 (*a*) A. Sarkar, T. Mukherjee and S. Kapoor, *J. Phys. Chem. C*, 2008, **112**, 3334–3340; (*b*) G. Jian, Y. Liu, X. He, L. Chen and Y. Zhang, *Nanoscale*, 2012, **4**, 6336–6342.

9 (*a*) E. R. Costa, F. C. D. Andrade, D. Y. de Albuquerque, L. E. M. Ferreira, T. M. Lima, C. G. S. Lima, D. S. A. Silva, E. A. Urquieta-González, M. W. Paixão and R. S. Schwab, *New J. Chem.*, 2020, **44**, 15046–15053; (*b*) P. Kalra, R. Kaur, G. Singh, H. Singh, G. Singh, G. Kaur and J. Singh, *J. Organomet. Chem.*, 2021, **944**, 121846; (*c*) B. Mondal, M. Kundu, S. P. Mandal, R. Saha, U. K. Roy, A. Roychowdhury and D. Das, *ACS Omega*, 2019, **4**, 13845–13852; (*d*) D. Ghosh, S. Dhibar, A. Dey, P. Manna, P. Mahata and B. Dey, *ChemistrySelect*, 2020, **5**, 75–82.

10 Z. Zhang, C. Dong, C. Yang, D. Hu, J. Long, L. Wang, H. Li, Y. Chen and D. Kong, *Adv. Synth. Catal.*, 2010, **352**, 1600–1604.

11 G. Fonder, I. Minet, C. Volcke, S. Devillers, J. Delhalle and Z. Mekhalif, *Appl. Surf. Sci.*, 2011, **257**(14), 6300–6307.

12 A. Corma, V. Fornés, L. Forni, F. Márquez, J. Martinez-Triguero and D. Moscotti, *J. Catal.*, 1998, **179**, 451.
13 (*a*) X. Huang, Y. Zhu, W. Yang, A. Jiang, X. Jin, Y. Zhang, L. Yan, G. Zhang and Z. Liu, *Molecules*, 2019, **24**, 3132; (*b*) V. Sudha, G. Murugadoss and R. Thangamuthu, *Sci. Rep.*, 2021, **11**, 3413.
14 W. N. P. van der Graaff, G. Li, B. Mezari, E. A. Pidko and E. J. M. Hensen, *ChemCatChem*, 2015, **7**, 1152.
15 D. Verboekend, G. Vilé and J. Pérez-Ramírez, *Cryst. Growth Des.*, 2012, **12**, 3123.
16 R. Hajjar, Y. Millot, P. P. Man, M. Che and S. Dzwigaj, *J. Phys. Chem. C*, 2008, **112**, 20167–20175.
17 A. M. Kłonkowski, B. Grobelna, T. Widernik, A. Jankowska-Frydel and W. Mozgawa, *Langmuir*, 1999, **15**, 5814–5819.
18 B. Andrews, S. Almahdali, K. James, S. Ly and K. N. Crowder, *Polyhedron*, 2016, **114**, 360–369.